Can co-activation reduce kinematic variability? A simulation study.

Selen, L.P.J.; Beek, P.J.; van Dieen, J.H.

published in
Biological Cybernetics
2005

DOI (link to publisher)
10.1007/s00422-005-0015-y

Biol Cybern (2005) 93: 373–381
DOI 10.1007/s00422-005-0015-y

ORIGINAL PAPER

Biological Cybernetics

Luc P.J. Selen · Peter J. Beek · Jaap H. van Dieën

Can co-activation reduce kinematic variability? A simulation study

Received: 1 April 2005 / Accepted: 1 August 2005 / Published online: 25 October 2005

Abstract Impedance modulation has been suggested as a means to suppress the effects of internal 'noise' on movement kinematics. We investigated this hypothesis in a neuro-musculo-skeletal model. A prerequisite is that the muscle model produces realistic force variability. We found that standard Hill-type models do not predict realistic force variability in response to variability in stimulation. In contrast, a combined motor-unit pool model and a pool of parallel Hill-type motor units did produce realistic force variability as a function of target force, largely independent of how the force was transduced to the tendon. To test the main hypothesis, two versions of the latter model were simulated as an antagonistic muscle pair, controlling the position of a frictionless hinge joint, with a distal segment having realistic inertia relative to the muscle strength. Increasing the impedance through co-activation resulted in less kinematic variability, except for the lowest levels of co-activation. Model behavior in this region was affected by the noise amplitude and the inertial properties of the model. Our simulations support the idea that muscular co-activation is in principle an effective strategy to meet accuracy demands.

1 Introduction

Human motor behavior is variable yet efficient. The variability is an inevitable consequence of the stochastic nature of neuromuscular processes. On the output side this is manifest in the variability of motor unit spiking behavior (e.g. Matthews 1996), isometric force (e.g. Jones et al. 2002), and movement kinematics (e.g. Scholz et al. 2000; Tseng et al. 2003).

Optimal control models have been used to study the relation between variability and task performance. Models of the noisy neuromotor system accurately replicate experimental data of saccades and arm movements when endpoint variance is minimized (Harris and Wolpert 1998; Hamilton and Wolpert 2002). When feedback is added, phenomena like task-constrained variability, goal-directed corrections and motor synergies emerge naturally from stochastic optimal control models (Todorov and Jordan 2002). A shortcoming of these models is that they are driven by pure force and moment actuators and thus ignore the impedance characteristics of the muscles (Osu et al. 2004).

Impedance modulation has been proposed as a means to reduce the contribution of force fluctuations to kinematic variability (Van Galen and De Jong 1995). This extra degree of freedom, which, in theory, can be controlled by co-activation of muscles (Osu and Gomi 1999), is supposed to act as a low-pass filter between the force fluctuations and movement kinematics. Burdet et al. (2001) measured hand path error and impedance of point-to-point movements before, during and after the exposure to a negative elastic force field perpendicular to the movement direction. To overcome the trajectory instability due to the force field, subjects increased the mechanical impedance of the arm. Interestingly, after removal of the force field the hand path error was smaller than in the trials prior to the exposure to the force field. Also the variability of jaw movements seems to be influenced by impedance modulations (Shiller et al. 2002). Studies on muscular co-activation have provided more direct evidence for impedance modulation in response to increased accuracy demands. Both in single-joint (Osu et al. 2004) and multi-joint (Laursen et al. 1998; Gribble et al. 2003; Visser et al. 2004) movements co-activation increases with accuracy demands.

The role of joint impedance to resist unpredictable external force perturbations has been investigated in both static (e.g. Perreault et al. 1999) and dynamic (e.g. Burdet et al. 2001; Franklin et al. 2003) tasks. On mechanical grounds it is obvious that excursions from the planned trajectory will decrease with increased impedance (Wagner and Blickhan 2003). For internal force fluctuations the role of impedance modulation is less straightforward because both muscular

L.P.J. Selen · P.J. Beek · J.H. van Dieën (✉)
Faculty of Human Movement Sciences and Institute for Fundamental and Clinical Human Movement Sciences, Vrije Universiteit, Van der Boechorststraat 9, 1081 BT Amsterdam, The Netherlands
E-mail: j.vandieen@fbw.vu.nl

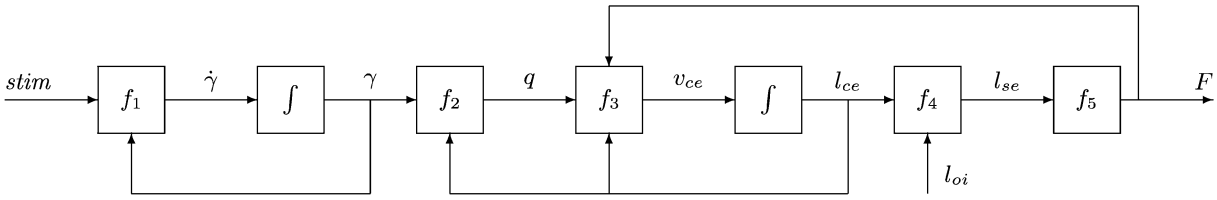

Fig. 1 Block diagram showing the flow of calculations in the lumped muscle models. The functions f_1 through f_5 are explained in the text. The integral signs indicate integration with respect to time. External inputs are the stimulation ($stim$) and the origin-insertion length (l_{oi}). $\dot{\gamma}$: calcium concentration change; γ: calcium concentration; q: active state; v_{ce}: contractile element velocity; l_{ce}: contractile element length; l_{se}: tendon length; F: muscle force. Two regimes of stimulus variability were simulated: continuous lumped model (CLM) and discrete lumped model (DLM)

force fluctuations (Jones et al. 2002; Christou et al. 2002) and joint impedance (Osu and Gomi 1999) increase linearly with muscular contraction levels. This creates the paradoxical situation that, on the one hand, the muscles are the source of the force fluctuations while on the other hand they could help suppress their effects by modifying joint impedance.

The goal of this paper is to elucidate the relations among force variability, impedance modulation and kinematic variability by examining how these relations might be implemented in a neuro-musculo-skeletal model. To anticipate, we show that standard Hill-type muscle models are inappropriate to simulate realistic force variability and that a more detailed description of muscular behavior and control is needed. In Sect. 3, this results in a model with multiple motor units, whose contraction dynamics are described by Hill-type muscle equations, and a motor unit pool as the control mechanism. Finally, we show that co-activation of muscles of the latter type does not necessarily result in larger kinematic variation in spite of increases in the force variability of the individual muscles.

2 Force variability in a standard Hill-type muscle model

2.1 Model and simulation

Our first goal was to obtain a formulation of a dynamic neuromuscular model that produces realistic isometric force variability. In most large scale musculo-skeletal models, muscle behavior is described by length-force and velocity-force equations (e.g. Pandy et al. 1990; Van Soest and Bobbert 1993). The characteristics of the individual fibers and motor units are lumped together in a single contractile element (CE) connected to a series elastic element (SE). These lumped models have proved suitable for deterministic simulations of maximal jumping (e.g. Pandy et al. 1990; Van Soest and Bobbert 1993) and ballistic arm movements (e.g. Welter and Bobbert 2002). In addition, they have been instrumental in showing that intrinsic muscle properties may compensate for errors in motor planning and small variations in initial conditions (Van Soest and Bobbert 1993; Wagner and Blickhan 2003; Van der Burg et al. 2005).

The question is whether these lumped models are also suitable to simulate realistic force variability. To answer this question, we examined the behavior of a model with excitation–activation–contraction dynamics as described in Van Soest and Bobbert (1993) and Ridderikhoff et al. (2004). We compared this with the experimental finding that isometric force variability, as indexed by its standard deviation (SD), increases monotonically with the mean (Christou et al. 2002; Jones et al. 2002; Taylor et al. 2003).

The flow of calculations is depicted in Fig. 1. Input to the model is the stimulation of the muscle ($stim$), a number between 0 and 1 representing both recruitment and rate coding. The calcium concentration (γ) is related to $stim$ by first order dynamics (f_1) with a time constant τ of 89 ms. The active state q was calculated from γ through a nonlinear equation (f_2), which also depends on CE length. Function f_3 represents the force-velocity and force-length relations. Contractile element velocity (v_{ce}) was calculated from CE length (l_{ce}), force and active state. Integration of v_{ce} resulted in the new l_{ce}, from which, in combination with the origin-insertion length (l_{oi}), the tendon length (l_{se}) was calculated (f_4). Finally, the muscle force was calculated from current SE length (f_5), modeled as a quadratic spring; see Table 1 and Ridderikhoff et al. (2004) for parameter values.

In order to create force variability, Gaussian distributed noise was introduced at the input stage of the model. The SD of this noise increased linearly with the mean value of $stim$, with a gain of 0.1. In other words, the noise had a constant coefficient of variation (CV) of 0.1. Two regimes were simulated: in the first regime, a new value for $stim$ was drawn from the Gaussian distribution every millisecond. An Euler–Maruyama integration scheme, suitable for studying stochastic differential equations, with a stepsize of 1 ms was used in the simulations. We refer to this model as the Continuous Lumped Model (CLM). In the second regime, the $stim$ value was kept constant over an interval based on the instantaneous firing rate. In this case the forward simulations were performed with a *normal* Euler integration scheme, again with a stepsize of 1 ms. This model will be referred to as the Discrete Lumped Model (DLM). We studied the output

Table 1 Muscle parameters

Parameter	Description	Value
F_{max}	Maximum total isometric force [N]	2000
$l_{ce,opt}$	Optimum fiber length [m]	0.136
$l_{se,slack}$	Tendon slack length [m]	0.170
a	Muscle moment arm [m]	0.03
I	Segment inertia [Nms^2/rad]	0.1

All other parameters are either mentioned in the text or are the same as in Ridderikhoff et al. (2004)

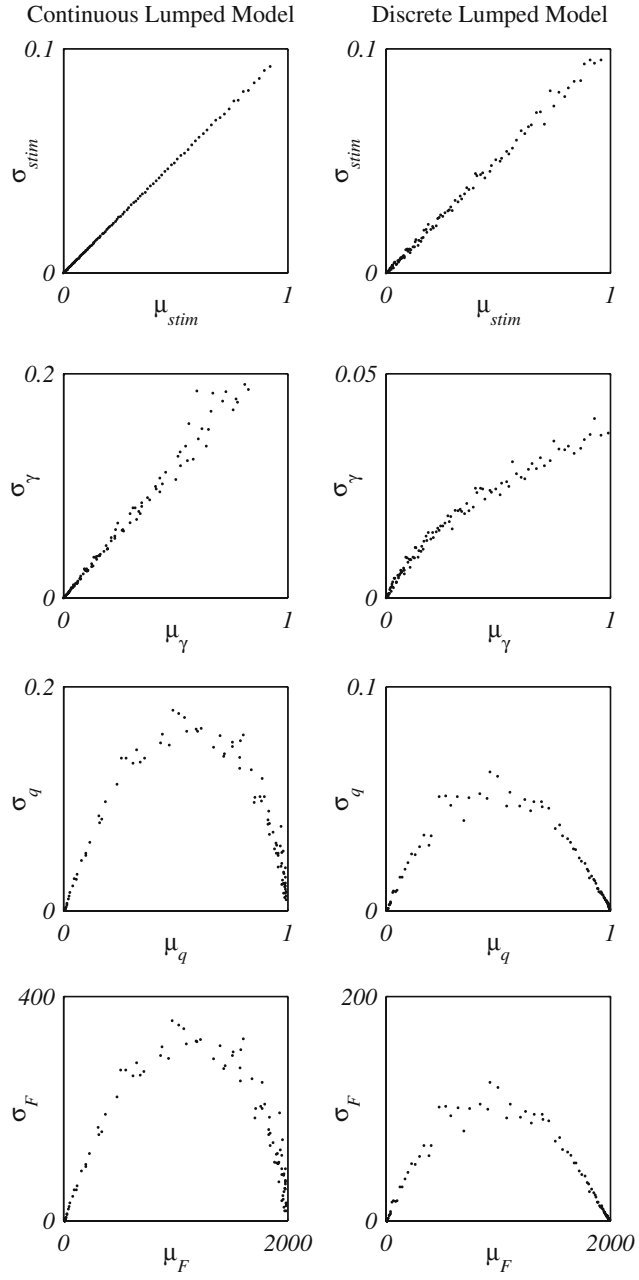

Fig. 2 The propagation of noise for increasing average levels of $stim$ in the CLM (left column) and the DLM (right column). Note the scale differences in γ, q and F. See text for model descriptions

variables γ, q and F and their variability for different values of $stim$. Time series of 15 s were simulated to quantify (force) variability.

2.2 Simulation results and discussion

Figure 2 shows how noise on $stim$ propagates through the muscle model with increasing mean levels of $stim$ for both the continuous (left) and the discrete (right) case. Every dot represents the mean and standard deviation of a 15 s simulation. The amplitude of the noise on $stim$ was the same in both models, whereas the DLM also contained noise in the timing. In the CLM every mean and SD is based on 15e3 drawings from a Gaussian distribution, whereas the number of drawings in the discrete model is approximately 30 times lower. This accounts for the larger variance in the simulation results of the DLM. The next row of Fig. 2 shows the variability in the calcium concentration. The curve for the continuous model is again linear, whereas that for the discrete model clearly is not. This difference is due to the frequency content of the time series. In the continuous case the frequency content is independent of $stim$, whereas in the discrete case the frequency content increases with higher $stim$. The first order dynamics between $stim$ and γ acts as a low pass filter and as a result the graph of μ_γ against σ_γ is less than linear. In the conversion from γ to q the monotonic relation of mean and standard deviation disappears and changes into a parabolic one. This parabolic relation persists in the force. In contrast, the standard deviation of the force has been shown experimentally to increase monotonically with mean force (Jones et al. 2002; Christou et al. 2002).

Although we can already conclude that the model is inadequate to answer our main question, it is informative to examine which properties of the model render it inadequate for this purpose. The force variability is mainly modulated by the filtering properties of the excitation ($stim$) to activation (q) coupling. Figure 3 shows the sigmoid relation between $stim$ and q (solid line) and explains how constant CV variation on $stim$ is heavily attenuated through this relation.

The present results suggest that the filtering properties of the lumped Hill model do not allow modeling of realistic variability in muscular force output. The formulation is a

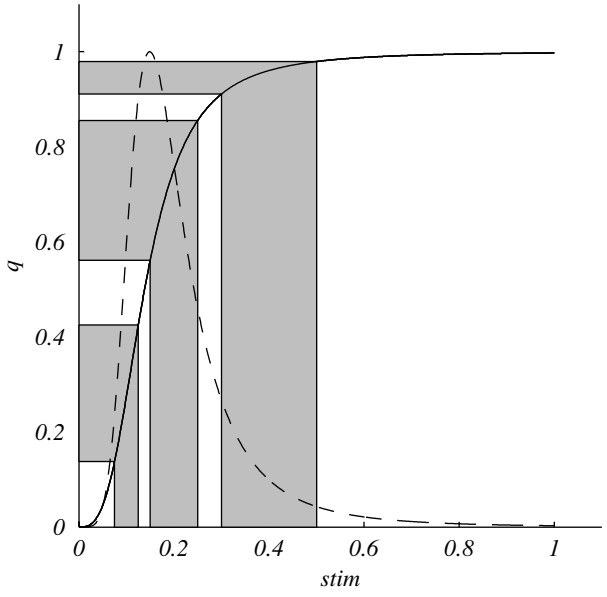

Fig. 3 Schematic representation of the noise suppression properties of the CLM. The solid curve represents the steady state relation between $stim$ and active state (q). The bands show the transfer of constant CV stimulus variability to active state variability. The dashed line represents $q \cdot dq/dstim$, which is the susceptibility of q to constant CV input noise

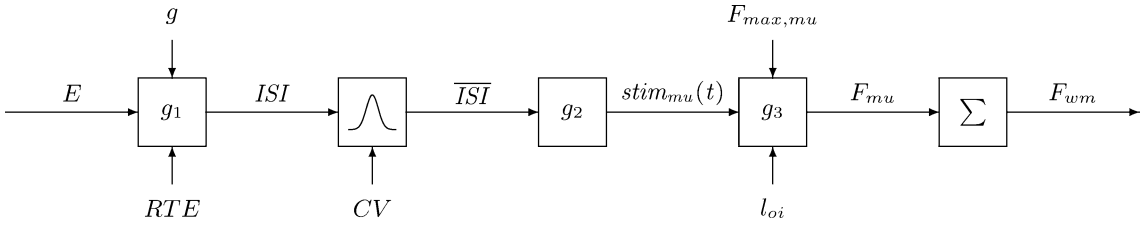

Fig. 4 Block diagram showing the flow of calculations in the multiple fibre muscle models. The functions g_1 through g_3 are explained in the text; g_3 comprises the flow diagram of Fig. 1. Two regimes were simulated: with independent tendons (ITM) and with dependent tendons (DTM) of the motor units. E: excitatory drive; ISI: interspike interval of m.u.; $\overline{ISI}$: Gaussian distributed interspike intervals; $stim_{mu}(t)$: stimulus of m.u.; F_{mu}: m.u. forces; F_{wm}: total force

description of average behavior of all motor units, leaving the processes underlying force variability unaddressed. Whereas the merits of this modeling approach in deterministic simulations are undisputed, it falls short as a basis for studying motor variability.

3 Force variability in a motor-unit pool model

3.1 Model and simulation

The organization of the motor-unit (MU) pool has been mentioned as the main source of isometric force variability (Jones et al. 2002). In the preceding model, the properties of the MU pool were lumped together in $stim$. Since this did not lead to a satisfactory result, the organization of the MU pool was modeled explicitly .

Figure 4 depicts the flow of calculations of the MU pool model. The motor-neuron pool, controlling the motor units, was inspired by the model presented by Fuglevand et al. (1993). Muscular force is modulated by two processes: the number of active motor units (recruitment) and the firing rate of these units (rate coding). In the original formulation, the outputs of the motor neuron pool were the time instances of the discharges. Upon discharge an MU twitch occurred. In our formulation, the motor neuron pool codes the value of $stim_{mu}$ and the time that this value remains constant. An MU is recruited when the excitatory drive (E_{pool}) exceeds the recruitment threshold (RTE). The RTEs of the different units are expressed as an exponential

$$\text{RTE}(mu) = \text{e}^{mu(\ln \text{RR})/n} \tag{1}$$

where mu is the index of the motor neuron, RR the recruitment range and n the number of motor units. In our simulations RR = 30 and $n = 60$ were used. Upon recruitment the motor neuron starts firing at its minimum firing rate (MFR) of 5 pps. The firing rate increases linearly with the excitatory drive. The gain (g) of this relation is 1.5. The firing rate increases until it saturates at 100 pps. Thus, the firing rate response of a motor neuron to a constant excitatory drive is:

$$\text{FR}_{mu} = g \cdot [E_{\text{pool}} - \text{RTE}_{mu}] + \text{MFR} \quad E_{\text{pool}} \geq \text{RTE}_{mu} \tag{2}$$

The inverse of the firing rate is the interspike interval ($\text{ISI}_{mu} = 1/\text{FR}_{mu}$). These calculations take place in box g_1 of Fig. 4. Fluctuations in the ISI due to membrane noise have a Gaussian distribution with a nearly constant CV (Matthews 1996). For our simulations we chose a CV of 0.2 (Adam et al. 1998). The ISI distributions were concatenated to time series of the spiking events of the different MUs. From the ISI we also calculated the normalized firing frequency, which was kept constant within the corresponding interspike interval (g_2; $stim_{mu}(t)$). The stimulation of a single MU ($stim_{mu}$) is now a representation of its firing rate only.

The maximal isometric force of each MU increased exponentially with the MU number (mu):

$$F_{max,mu} = c \cdot \text{e}^{mu \cdot \ln(\text{RF})/n} \tag{3}$$

where RF is the range of forces in the pool. In our model the last recruited MU had a maximal force of 30 times the maximal force of the first recruited unit. The parameter c was chosen such that the maximal isometric force of the whole muscle was 2000 N.

Two models of the contraction dynamics were formulated (g_3). In the first model every MU, i.e. a lumped cluster of fibers, is described by the equations of the model in Sect. 2. The motor units act independently of one another except for their l_{oi}, resulting in a distribution of l_{ce} and l_{se}. We refer to this model as the independent tendon model (ITM). The second model represents the other extreme of interdependency. All contractile elements attach to the same tendon and all have the same l_{ce} and v_{ce}. We refer to this model as the dependent tendon model (DTM). For this model there is no analytic solution for v_{ce} as a function of F_{ce} and q. In the ITM, F_{ce} equals F_{se}. In the DTM, we only know that the sum of all F_{ce} equals F_{se}. An iterative minimization of $(\sum_1^{nMU} F_{\text{ce}}(v_{\text{ce}}) - F_{\text{se}})^2$ at every time step of the simulation was used to find the solution; see Table 1 for the contraction model parameters.

Output variables we looked at were: $stim$, γ, q and F of the individual motor units and their variability for different values of E_{pool}. The main output parameter was the total force of the muscle (F_{wm}). All calculations were based on 15 s time series, which were obtained by Euler integration of the model equations with a timestep of 1 ms.

3.2 Simulation results and discussion

Figure 5 shows how SD of total muscle force increases with increasing average simulated whole muscle force, for

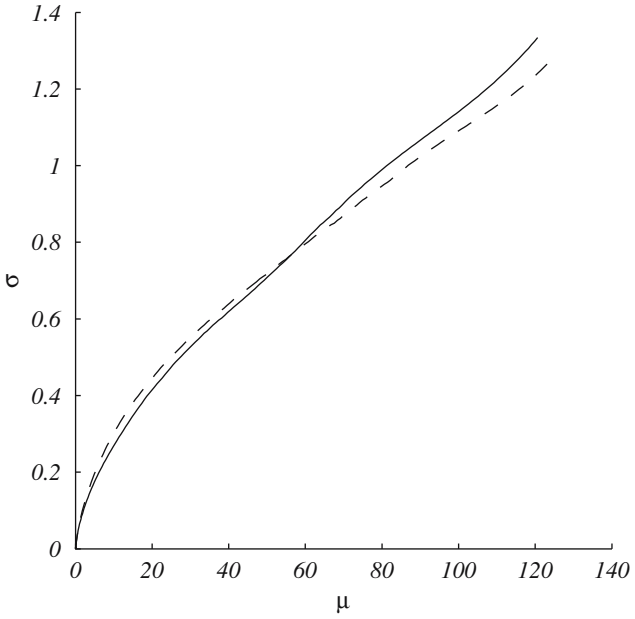

Fig. 5 Force variability, expressed as the SD (σ), as a function of the average force (μ). Continuous line for the ITM and dashed line for the DTM. The origin-insertion length (l_{oi}) was $0.75 \cdot l_{\text{oi,opt}}$

$l_{\text{oi}} = 0.75 \cdot l_{\text{oi,opt}}$. The results for $l_{\text{oi}} = 0.95 \cdot l_{\text{oi,opt}}$ were similar. The force variability increases with the average force. The variability was between 1 and 10% of the average force. This is in accordance with the experimental values of 2–10% (Adam et al. 1998; Laidlaw et al. 2000; Jones et al. 2002; Taylor et al. 2003). In the literature there is no consensus about the shape of force variability curves. All studies report a monotonically increasing SD with mean force, but the exact relation is either sigmoid (Slifkin and Newell 1999; Christou et al. 2002), linear (Jones et al. 2002) or less than linear (decreasing CV, (Laidlaw et al. 2000)).

Figure 6 shows how increasing E_{pool} affects the behavior of the individual motor units. Essentially, the behavior of the individual units is the same as the behavior of the DLM. For clarity only motor units 1, 20, 35 and 50 are shown, at an l_{oi} of $0.75 \cdot l_{\text{oi,opt}}$. For $stim$, γ and q the ITM and DTM do not differ markedly and we will discuss them together. In the μ_{stim}-curves we recognize Eq. 2 with different RTE for the units and a gain of 1.5. Although the model was constructed to saturate at 1, the stochastic model saturates at a lower value. One can understand this from cutting off the Gauss distribution when approaching the saturation value of 1. This also accounts for the drop and saturation in the σ_{stim} curves. The second row presents the calcium concentration γ. First order dynamics link γ and $stim$. Therefore μ_γ reacts exactly the same to E_{pool} as μ_{stim}. Increasing E_{pool} results in a shift of the main frequency of $stim$. The low-pass filtering properties of the excitation dynamics now suppress the variability of γ (See also Sect. 2). The third row presents the active state q. The relation between E_{pool} and q is sigmoid and therefore σ_q drops after μ_q exceeds 0.5.

From the forces depicted in the fourth row we observe that the largest contribution to the force comes from the last recruited units. More importantly, also the force variability is mainly determined by the last recruited MUs. The relative contribution of every MU to the total force and the total force variability is determined by the number of MUs (nmu), the range of MU forces (RF) and the recruitment range (RR) in Eqs. 1, 2, and 3. The values used in this study are within the physiologic range and changes only mildly alter model behavior.

Furthermore, several differences between the ITM and DTM come to the fore. In the ITM, μ_F of the individual units saturates, whereas in the DTM the force reaches a peak and then slightly decreases. In the ITM, the l_{ce} of the MUs is fixed after having reached maximum activation. In the DTM, the l_{ce} is not only determined by the activation of the unit itself, but also by the activation of the surrounding units. This is reflected as a higher variability of the DTM in the low force range and a lower variability in the high force range compared to the ITM (Fig. 5).

In conclusion, both the ITM and the DTM exhibit realistic force variability. The models are at the extremes of motor unit interdependency and will be used in addressing the issue of kinematic stability.

4 Kinematic stability of the motor-unit pool model

4.1 Model and simulation

In order to investigate the relation between force variability, co-activation, impedance and kinematic variability, two neuro-musculo-*skeletal* models were constructed with respectively the ITM and DTM as actuators (see Fig. 7). The planar skeletal model comprised an inertia, connected to the stationary world by means of a frictionless hinge joint. Two antagonistic muscles modeled as in Sect. 3 were connected to the inertia. In addition to the forces, the neuro-muscular models also provide the model with stiffness and damping resulting from their length-force and velocity-force relations. No passive stiffness and damping were included. The only objective was to show that co-activation can in principle be an effective strategy to reduce kinematic variability. With no particular joint in mind, the model was symmetric and the moment arms of the muscles were constant; see Table 1 for the values used. The parameters of the muscles and the inertia are in the range of those known for the lower arm.

The model was simulated at an equilibrium angle of 0 (symmetric case) and 10 (asymmetric case) degrees. The latter value was chosen to investigate the effects of asymmetric muscle length and activation. Again, time series of 15 s were simulated with an Euler integration scheme. Output parameters were the joint angle and the forces of the individual muscles. Co-activation level was expressed as the E_{pool} value of the most active muscle.

Additional simulations were performed to reveal the impedance characteristics of the models. The model was perturbed by a simulated external torque pulse of 1 Nm. The impedance was estimated by calculating $dM/d\varphi$ over the first 10 ms after perturbation onset.

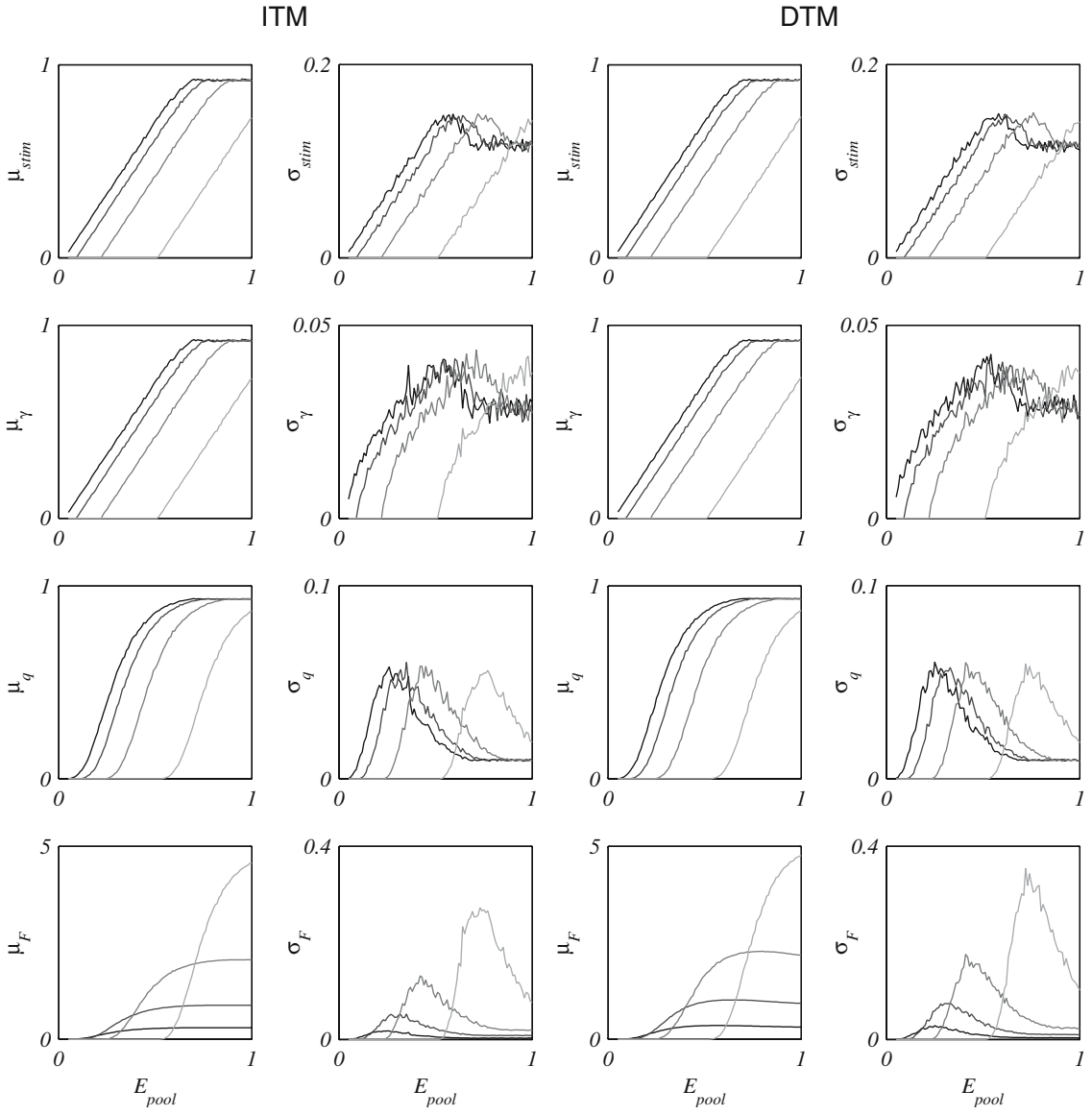

Fig. 6 The influence of ISI variability of motor units 1, 20, 35, and 50 on individual motor-unit behavior in the ITM (columns 1 and 2) and the DTM (columns 3 and 4). l_{oi} was $0.75 \cdot l_{\mathrm{oi,opt}}$. Average behavior (columns 1 and 3) and variability (column 2 and 4) of the individual motor units are presented as a function of E_{pool} for the excitation ($stim$), the calcium concentration (γ), the active state (q) and the force (F). See main text for model descriptions and discussion

4.2 Simulation results and discussion

Figure 8 shows the kinematic variability, expressed as the SD of the joint angle, as a function of the co-activation level, in the symmetric case for both the ITM and DTM. Both models show a peak in the kinematic variability, irrespective of model asymmetry (not shown in the figure). These peaks are a consequence of two competing factors: force variability and impedance. Figure 9 illustrates the results of simulations of an external perturbation. The left panel shows how the impedance changes with the co-activation level. The force variability increase with co-activation is similar to that in the isometric contractions (Sect. 3, Fig. 5). Without impedance, the increasing force variability would bring about ever larger kinematic fluctuations, as is visible at low co-activation levels in Fig. 8. The increasing impedance due to co-activation attenuates this effect and eventually decreases the kinematic variability although the force variability still increases.

The above explanation implies that increasing the inertia of the system would shift the peak kinematic variability to higher co-activation values. Furthermore, introducing more force variability, for instance by introducing noise in E_{pool}, would shift the peak kinematic variability to lower values of co-activation and eventually lead to a monotonically decreasing kinematic variability as a function of co-activation. The ITM was put to the test for both manipulations of the model (see Fig. 10) and our expectations were indeed confirmed. The effect of a 10-fold inertia increase was only

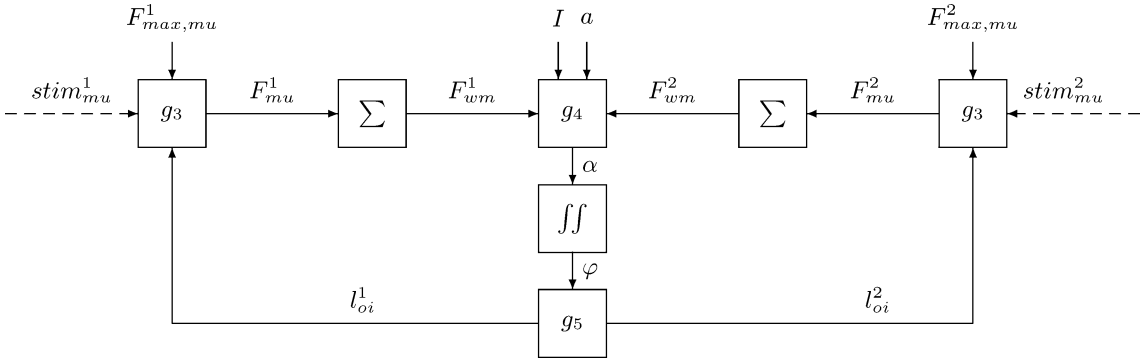

Fig. 7 Block diagram showing the flow of calculations for the kinematic stability simulations. The $stim_{mu}$ come from the alpha motor neuron pools of the individual muscles as described in Sect. 3. The function g_3 comprises the block diagram of Fig. 1 and calculates the individual m.u. forces (F_{mu}), given the origin-insertion length (l_{oi}). Summation results in the whole muscle forces (F_{wm}), the net of which moment results in an angular acceleration of the inertia (g_4, inputs I (inertia) and a (moment arms)), leading to an angular displacement (φ). This angular displacement creates a negative feedback loop via the l_{oi} of the individual muscles

diminutive, suggesting that the model is rather insensitive to inertia changes. On the other hand, the addition of noise in E_{pool} changes the overall properties of the model and results in a monotonic decrease of kinematic variability with co-activation level.

Based on isometric force variability, we were unable to distinguish between the ITM and the DTM. As regards the kinematic variability there is a marked difference between both models. Especially in the low co-activation range, the DTM shows less kinematic variability than the ITM. The force variability of the two models was not markedly different, suggesting that impedance is the key factor. Nevertheless, from the co-activation versus impedance curves (left panel Fig. 9) no clear distinction can be made. When we look at the relative impedance (right panel Fig. 9) we see that DTM is much stiffer than the ITM, especially at low co-activation levels. This accounts for the differences in the kinematic variability between the ITM and the DTM. In reality the mechanical interaction between MUs will be somewhere in between the two models.

How the modulation of muscular co-activation affects kinematic variability depends, according to our model, particularly on the central and peripheral noise levels in the neural system and the mechanical interactions of individual MUs within a muscle and the mechanical interactions between muscles.

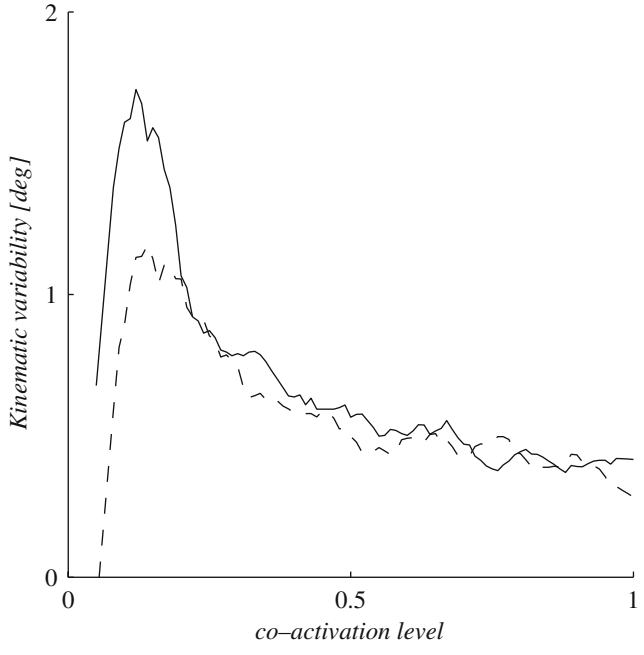

Fig. 8 Kinematic variability as a function of co-activation level for the symmetric model. *Continuous lines* for the ITM and *dashed lines* for the DTM. The kinematic variability is expressed as the SD of the joint angle

5 General discussion and conclusions

Our first concern in the present study was to build a model of muscular contraction, and thus force generation that produces realistic force variability. Prior attempts to simulate force variability were all based on motor unit pool models in combination with twitch forces (Van Galen and De Jong 1995; Jones et al. 2002; Taylor et al. 2003). These models revealed that the architecture of the MU pool plays a key role in force variability. We came to the same conclusion: The

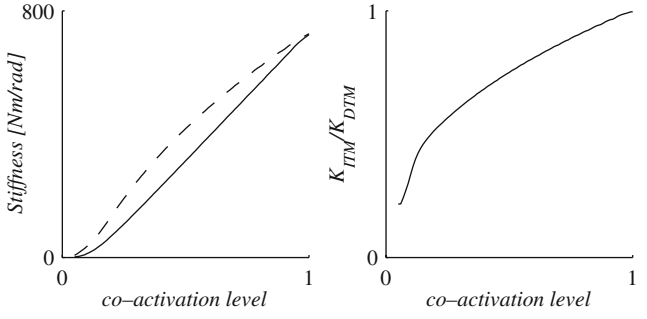

Fig. 9 Left: Stiffness estimate of the symmetric ITM (*continuous*) and DTM (*dashed*) obtained from simulations of an external perturbation to the inertia. Right: Relative stiffness (K_{ITM}/K_{DTM})

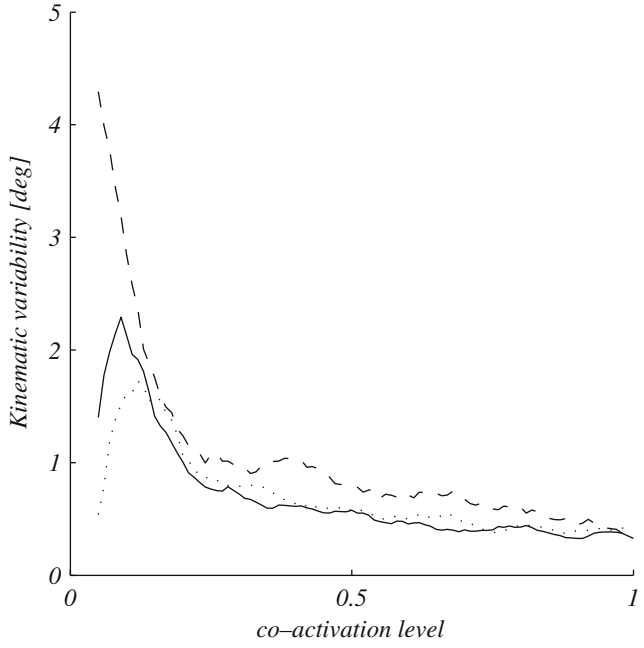

Fig. 10 Excitation (E_{pool}) variability and inertia manipulations in the ITM. Excitation variability was enhanced by introducing signal dependent noise (CV=0.2) in E_{pool} (*dashed line*, $CV = 0.2$). The *dotted line* represents results for a model without noise on E_{pool} and an inertia 10 times that in the standard model. The *solid line* represents the standard model

discrete nature of force generation and the MU pool architecture are essential ingredients to generate force variability. However, contrary to previous efforts, we included a contraction model. In this approach, the force is not only a function of the stimulation but also of muscle length and contraction velocity. With regard to force variability, this addition does not significantly affect the results, but the extended model allowed us to study the effects of force fluctuations on kinematic variability.

The relation between variability and motor control has recently been extensively studied in the field of computational motor control (Harris and Wolpert 1998; Hamilton and Wolpert 2002; Todorov and Jordan 2002). Continuous stochastic optimal control strategies resulted in model behavior that resembled experimental findings. Although these models provide clues about what the neural system is controlling, our results reveal some important shortcomings. First, the discrete nature of information processing influences the variability characteristics of the forces. Second, as was demonstrated here, these models lack antagonistic muscle function. Antagonistic muscles might act as a mechanical filter in that they may suppress, through co-activation, the effects of force variability on kinematic variability.

Combining a MU-pool model with a model of muscular contraction dynamics is a means to incorporate impedance into the model. The importance of adding contraction dynamics to the motor-unit pool model is manifest in the relation between force variability and kinematic variability. Net moment changes due to force fluctuations of the individual muscles are attenuated and eventually suppressed by the intrinsic stabilizing properties (impedance) of the antagonistic muscles. In reality, reflex components also contribute to joint dynamics in postural tasks. Reflexes contribute to the movements of the lower extremities in gait (e.g. Mazzaro et al. 2005). For the upper extremity such contributions are unlikely because external perturbing contact forces are absent. In the upper extremity, reflexes are likely required to overcome drift from the desired trajectory or position, which in a limited number of simulations occurred. Further research into the function of (noisy) spindle and Golgi-tendon feedback loops during, externally, unperturbed movements is needed. For now we want to stress that MU activation is the final common path of both central and peripheral inputs and determines force and moment fluctuations.

In the literature it has been suggested that kinematic variability decreases monotonically with co-activation (Van Galen and De Jong 1995). Especially in the low co-activation range, our model is sensitive to the choice of parameters in model simulations of this hypothesis. However, our simulations started at zero levels of activation. This is unrealistic given the presence of gravity. As a result humans seldom act in the lowest co-activation range of our model. Moreover, when noise was added to the central commands a monotonic relation emerged, implying that in practice a monotonic relation between co-contraction and kinematic variability for the lower co-contraction range can be expected. Only very recently has our assumption of constant CV over the range of interspike intervals been refuted (Moritz et al. 2005). The CV was found to decrease exponentially over the force range. Implementation of this fact in the model will probably also direct the model to monotonically decrease kinematic variability with co-activation. At high co-activation levels, the kinematic variability of our model stabilizes. In reality, synchronization might occur at high co-activation levels, possibly leading to an increase in force variability, which becomes apparent as tremor (i.e. kinematic variability in a specific frequency band (e.g. McAuley et al. 1997)).

The ITM and DTM represent two extreme cases of interdependency of the MUs, and thus of muscle impedance. In reality, the interdependency of the MUs will fall in between the ITM and DTM. Differences in kinematic variability between the ITM and DTM are only prominent at low levels of stimulation. This is, however, the working range for most tasks in daily life. But, as we stated before, model behavior is also influenced by several other (neural) factors in this region and a deliberate classification of their importance cannot be made at the moment.

This study underscores that the strategy of the neural system to control the effects of force variability on kinematic variability strongly depends on neural noise levels and sources, muscular architecture and skeletal properties. As such, it represents a first step in understanding how energetic and accuracy constraints might interfere within the motor control system.

References

Adam A, De Luca CJ, Erim Z (1998) Hand dominance and motor unit firing behavior. J Neurophysiol 80(3):1373–1382

Burdet E, Osu R, Franklin DW, Milner TE, Kawato M (2001) The central nervous system stabilizes unstable dynamics by learning optimal impedance. Nature 414(6862):446–449

Christou EA, Grossman M, Carlton LG (2002) Modeling variability of force during isometric contractions of the quadriceps femoris. J Mot Behav 34(1):67–81

Franklin DW, Burdet E, Osu R, Kawato M, Milner TE (2003) Functional significance of stiffness in adaptation of multijoint arm movements to stable and unstable dynamics. Exp Brain Res 151(2):145–157

Fuglevand AJ, Winter DA, Patla AE (1993) Models of recruitment and rate coding organization in motor-unit pools. J Neurophysiol 70(6):2470–2488

Gribble PL, Mullin LI, Cothros N, Mattar A (2003) A role for cocontraction in arm movement accuracy. J Neurophysiol 89(5):2396–2405

Hamilton AF, Wolpert DM (2002) Controlling the statistics of action: obstacle avoidance. J Neurophysiol 87(5):2434–2440

Harris CM, Wolpert DM (1998) Signal-dependent noise determines motor planning. Nature 394(6695):780–784

Jones KE, De AF, Hamilton C, Wolpert DM (2002) Sources of signal-dependent noise during isometric force production. J Neurophysiol 88(3):1533–1544

Laidlaw DH, Bilodeau M, Enoka RM (2000) Steadiness is reduced and motor unit discharge is more variable in old adults. Muscle Nerve 23(4):600–612

Laursen B, Jensen BR, Sjogaard G (1998) Effect of speed and precision demands on human shoulder muscle electromyography during a repetitive task. Eur J Appl Physiol Occup Physiol 78(6):544–548

Matthews PB (1996) Relationship of firing intervals of human motor units to the trajectory of post-spike after-hyperpolarization and synaptic noise. J Physiol 492(Pt 2):597–628

Mazzaro N, Grey MJ, Sinkjaer T (2005) Contribution of afferent feedback to the soleus muscle activity during human locomotion. J Neurophysiol 93(1):167–177

McAuley JH, Rothwell JC, Marsden CD (1997) Frequency peaks of tremor, muscle vibration and electromyographic activity at 10 hz, 20 hz and 40 hz during human finger muscle contraction may reflect rhythmicities of central neural firing. Exp Brain Res 114(3):525–541

Moritz CT, Barry BK, Pascoe MA, Enoka RM (2005) Discharge rate variability influences the variation in force fluctuations across the working range of a hand muscle. J Neurophysiol 93(5):2449–2459

Osu R, Gomi H (1999) Multijoint muscle regulation mechanisms examined by measured human arm stiffness and emg signals. J Neurophysiol 81(4):1458–1468

Osu R, Kamimura N, Iwasaki H, Nakano E, Harris CM, Wada Y, Kawato M (2004) Optimal impedance control for task achievement in the presence of signal-dependent noise. J Neurophysiol 92(2):1199–1215

Pandy MG, Zajac FE, Sim E, Levine WS (1990) An optimal control model for maximum-height human jumping. J Biomech 23(12):1185–1198

Perreault EJ, Kirsch RF, Acosta AM (1999) Multiple-input, multiple-output system identification for characterization of limb stiffness dynamics. Biol Cybern 80(5):327–337

Ridderikhoff A, Peper CL, Carson RG, Beek PJ (2004) Effector dynamics of rhythmic wrist activity and its implications for (modeling) bimanual coordination. Hum Mov Sci 23(3-4):285–313

Scholz JP, Schöner G, Latash ML (2000) Identifying the control structure of multijoint coordination during pistol shooting. Exp Brain Res 135(3):382–404

Shiller DM, Laboissiere R, Ostry DJ (2002) Relationship between jaw stiffness and kinematic variability in speech. J Neurophysiol 88(5):2329–2340

Slifkin AB, Newell KM (1999) Noise, information transmission, and force variability. J Exp Psychol Hum Percept Perform 25(3):837–851

Taylor AM, Christou EA, Enoka RM (2003) Multiple features of motor-unit activity influence force fluctuations during isometric contractions. J Neurophysiol 90(2):1350–1361

Todorov E, Jordan MI (2002) Optimal feedback control as a theory of motor coordination. Nat Neurosci 5(11):1226–1235

Tseng YW, Scholz JP, Schöner G, Hotchkiss L (2003) Effect of accuracy constraint on joint coordination during pointing movements. Exp Brain Res 149(3):276–288

Van der Burg JCE, Casius LJR, Kingma I, Van Dieën JH, Van Soest AJ (2005) Factors underlying the perturbation resistance of the trunk in the first part of a lifting movement. Biol Cybern 93(1):54–62

Van Galen GP, De Jong W (1995) Fitts' law as the outcome of a dynamic noise filtering model of motor control. Hum Mov Sci 12:539–571

Van Soest AJ, Bobbert MF (1993) The contribution of muscle properties in the control of explosive movements. Biol Cybern 69(3):195–204

Visser B, De Looze M, De Graaff M, Van Dieën J (2004) Effects of precision demands and mental pressure on muscle activation and hand forces in computer mouse tasks. Ergonomics 47(2):202–217

Wagner H, Blickhan R (2003) Stabilizing function of antagonistic neuromusculoskeletal systems: an analytical investigation. Biol Cybern 89(1):71–79

Welter TG, Bobbert MF (2002) Initial arm muscle activation in a planar ballistic arm movement with varying external force directions: a simulation study. Motor Control 6(3):217–229